

Ferromagnetic GeMn thin film prepared by ion implantation and ion beam induced epitaxial crystallization annealing

C. H. Chen, H. Niu, D. C. Yan, H. H. Hsieh, C. P. Lee, and C. C. Chi

Citation: *Applied Physics Letters* **100**, 242412 (2012); doi: 10.1063/1.4729752

View online: <http://dx.doi.org/10.1063/1.4729752>

View Table of Contents: <http://scitation.aip.org/content/aip/journal/apl/100/24?ver=pdfcov>

Published by the *AIP Publishing*

Articles you may be interested in

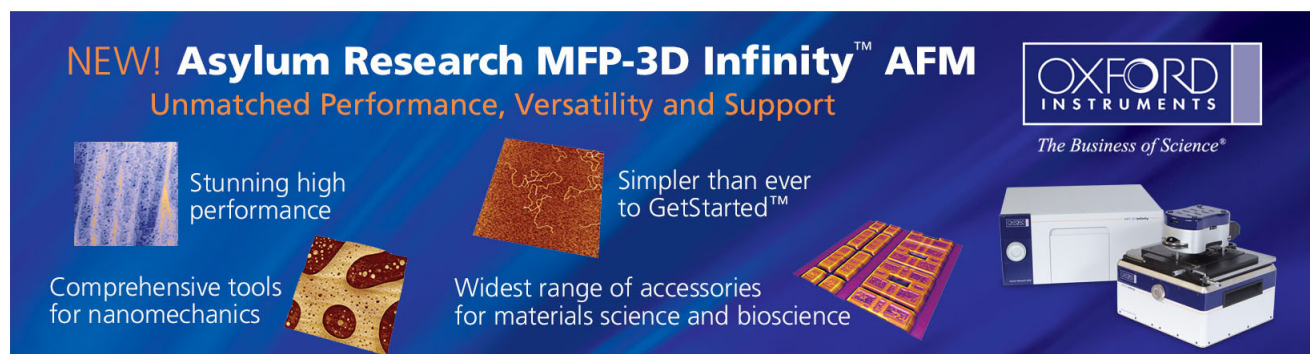
Enhanced magnetic and electrical properties in amorphous Ge:Mn thin films by non-magnetic codoping
J. Appl. Phys. **111**, 033916 (2012); 10.1063/1.3679076

Effect of annealing on the magnetic properties of Gd focused ion beam implanted GaN
Appl. Phys. Lett. **91**, 072514 (2007); 10.1063/1.2770762

Ferromagnetism and colossal magnetic moment in Gd-focused ion-beam-implanted GaN
Appl. Phys. Lett. **89**, 062503 (2006); 10.1063/1.2267900

Ferromagnetism and anomalous Hall effect in $\text{Co}_x\text{Ge}_{1-x}$
Appl. Phys. Lett. **89**, 042504 (2006); 10.1063/1.2236266

Carrier-induced ferromagnetism in Ge(Mn,Fe) magnetic semiconductor thin-film structures
Appl. Phys. Lett. **88**, 222508 (2006); 10.1063/1.2208552



NEW! Asylum Research MFP-3D Infinity™ AFM
Unmatched Performance, Versatility and Support

OXFORD INSTRUMENTS
The Business of Science®

Stunning high performance
Simpler than ever to GetStarted™
Comprehensive tools for nanomechanics
Widest range of accessories for materials science and bioscience

The advertisement features several images: a blue textured surface, a brown textured surface, a grid of colorful rectangular samples, and the Asylum Research MFP-3D Infinity AFM instrument.

Ferromagnetic GeMn thin film prepared by ion implantation and ion beam induced epitaxial crystallization annealing

C. H. Chen,¹ H. Niu,² D. C. Yan,³ H. H. Hsieh,⁴ C. P. Lee,¹ and C. C. Chi³

¹Center for Nano Science and Technology, National Chiao Tung University, Hsin Chu 30010, Taiwan

²Nuclear Science and Technology Development Center, National Tsing Hua University, Hsin Chu 30013, Taiwan

³Department of Physics, National Tsing Hua University, Hsin Chu 30013, Taiwan

⁴Department of Electrical Engineering, Chung Cheng Institute of Technology, Ta-shi, Tao-yuan 335, Taiwan

(Received 8 March 2012; accepted 1 June 2012; published online 15 June 2012)

Ferromagnetic GeMn was prepared by Mn implantation followed by ion beam-induced epitaxial crystallization annealing. The damage caused by Mn implantation was repaired by subsequent helium ion irradiation. Various structural analyses were performed and Mn ions were found to incorporate uniformly into the Ge lattice without the formation of any secondary phases. The remnant magnetic moment exhibited room temperature ferromagnetism. Anomalous Hall effect and field dependent magnetization were measured at the same time at room temperature indicating spin polarized free carrier transport. Additional measurement using x-ray magnetic circular dichroism also revealed that the carriers were spin-polarized. © 2012 American Institute of Physics. [<http://dx.doi.org/10.1063/1.4729752>]

Since the discovery of ferromagnetic ordering of InMnAs,¹ diluted magnetic semiconductors (DMS)^{1–3,28,29} have attracted considerable attention because of their potential applications in spintronics. GeMn, a group-IV DMS, has received considerable attention in recent years because of its compatibility with mainstream silicon technology.^{3–7} Over the years, several research groups have attempted to prepare ferromagnetic GeMn thin films using various methods.^{5,7–10} Although these samples exhibited ferromagnetic ordering,^{4,5,11–13,30} it was difficult to form a connection between the magnetic properties and the electronic transport properties.¹⁴

Intrinsically GeMn is less stable than GaMnAs. Because of limited solid solubility of Mn in Ge, GeMn thin films have to be prepared in a non-equilibrium way such as by low temperature-MBE growth or by ion-implantation. Even so, phase separation resulting in nano-metal cluster formation can easily happen when samples are subject to elevated temperature processes.^{9,12,13,15–17} Once secondary phase clusters are formed in the Ge matrix, it is difficult to remove them by conventional post-annealing processes.

Ion implantation is a convenient method in incorporating impurities into semiconductors at non-equilibrium conditions. However, thermal annealing process is usually needed to repair the damage in the crystal caused by implantation. For GeMn thin films, post-annealing has to be done in a very short time to prevent Mn atoms from being gathering and precipitating into clusters. Scarpulla *et al.*¹⁸ and Zhou *et al.*^{10,19} have demonstrated the use of pulsed laser annealing to form GaMnAs and GeMn thin films.

In this study, we prepared ferromagnetic GeMn films using ion beam-induced epitaxial crystallization (IBIEC) annealing after Mn implantation.^{20,21,31} The GeMn films prepared this way are extremely stable without any evidence of phase separation. The ferromagnetic properties were measured at room temperature. The anomalous Hall effect was observed at the same time and correlated very well with the magnetization measurement.

In IBIEC annealing, light ions are used to irradiate a previously implanted crystal to repair the damage.²¹ Part of the energy from the incident ions is transferred by nuclear stopping power to the dislocated host atoms to restore the crystallinity. In this work, we choose helium ions, which are light enough to go deep and at the same time to minimize the surface layer damage, which is usually a problem when heavy ion beam irradiation is used.

Mn-implantation was performed on *p*-type (001) Ge wafers, which were doped with Ga at a concentration of $1.1 \times 10^{18} \text{ cm}^{-3}$. To form a uniform Mn distribution in the implanted region, we implanted Mn⁺ ions with multiple energies of 70, 120, 170, 250, and 350 keV. Several samples were prepared with a total implanted dose varied from 5.5×10^{14} to $2.2 \times 10^{16} \text{ cm}^{-2}$, which corresponds to a Mn atomic percentage of 0.125% to 5.0% in the implanted region. The substrate was maintained at room temperature during implantation to prevent secondary phase formation. IBIEC treatment was then carried out using He ions at a beam current of $0.4 \mu\text{A cm}^{-2}$ with an energy of 350 keV for 2 h. During IBIEC treatment, the substrate was kept at a constant temperature of 523 K. After IBIEC, the samples were slightly etched in a NaOH + H₂O₂ solution to remove any possible oxide layer that may have formed during the implantation processes. Magneto-transport properties were measured using a Hall bar structure with the magnetic field applied perpendicularly to the sample surface. To understand the electronic structure of the prepared GeMn thin films, we used x-ray circular dichroism^{32,33} (XMCD), with measurement taken at the National Synchrotron Radiation Research Center, to analyze possible crystal formation of GeMn and the spin polarization of its carriers. The XMCD was performed at 78 K.

The structure of GeMn and the distribution of Mn were analyzed by double crystal x-ray diffraction (DCXRD) and SIMS. The Cu_{K α 1} x-ray (0.1542 nm) was selected by double Si(111) single crystals. The XRD spectra of the GeMn thin

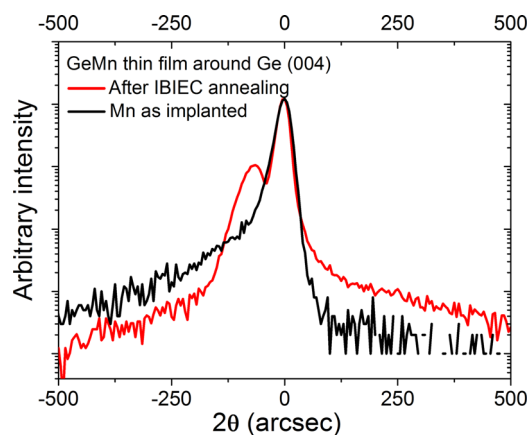


FIG. 1. DCXRD ω - 2θ scan revealing the formation of GeMn at the low angle side of Ge (004) peak after IBIEC annealing.

film around the (004) peak before and after IBIEC annealing are displayed in Fig. 1. Only one broadened peak was observed for the as-implanted sample indicating the Ge crystal had been damaged during Mn implantation. After IBIEC annealing, however, an additional shoulder peak appeared on the smaller angle side of the Ge (004) peak. This is a clear indication of the formation of a compressively strained GeMn film. The IBIEC treatment has caused the damaged Ge to recrystallize. But, because the smaller Mn atoms sit on the substitutional sites, the GeMn film is compressively strained. We have also checked Ge(224) and Ge(311) peaks, and similar shoulder peaks were observed. The formation of the compressively strained GeMn film was also confirmed by a separate study using XAFS.²² To make sure there was no secondary phase formation, we carefully scanned the XRD spectrum, even in logarithmical scale, using grazing incident x-ray diffraction. All the IBIEC annealed GeMn samples showed highly crystallized structure without the formation of secondary phases.^{9,13,16,23} We have also performed a cross-sectional TEM study of a sample before and after IBIEC treatment (see supplementary material for high resolution TEM pictures³⁴). Figure 2 shows the TEM picture of IBIEC annealed sample. The clear selected area diffraction (SAD) points shows that the amorphous region caused by Mn implant was repaired and the crystal lattice was restored.

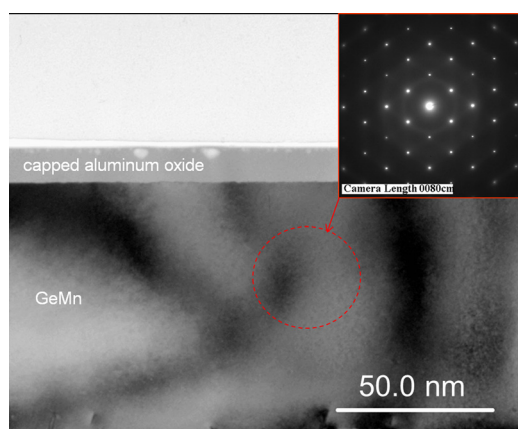


FIG. 2. The TEM images of IBIEC-annealed Ge:Mn sample, the inset is the SAD pattern which is selected from the regrowth area.

Time-of-flight secondary ion mass spectrometry (SIMS) was used to determine Mn distribution in Ge shows the measured Mn profiles for samples with various Mn doses before and after IBIEC treatment (also see supplementary material for SIMS profiles³⁴). The SIMS profiles do not actually change after IBIEC and are generally very similar to one another. This implies that the Mn atoms stayed where they were implanted during the IBIEC induced recrystallization process and the formation of the GeMn alloy, clearly indicating no Mn segregation took place. This is quite different from the results obtained using conventional thermal annealing techniques,^{24,25} where serious secondary phase precipitation usually takes place. The actual total Mn implanted doses calculated from the SIMS profiles were found to be in good agreement with intended implanted doses.

The magnetic properties of Mn-implanted samples were measured using a superconducting quantum interference device magnetometer (SQUID). Figure 3 shows the measured magnetization as a function of magnetic field at 5 K and 300 K for a 5% Mn sample. The diamagnetic background was subtracted from the data. Clear ferromagnetic behavior was observed. Elongated hysteresis loops are also visible in the figure. Figure 4 shows the remnant magnetic moment, measured after a 1 T-field was applied and then removed at low temperature, as a function of temperature. These results indicate that the IBIEC-annealed Mn-implanted samples have ferromagnetism above room temperature.

One of the most important criteria for DMS to be used in spintronics applications is to have a spin polarized transport property. The ferromagnetic behavior of the material has to be able to mediate the formation of spin polarization for the free carriers. In the past, however, such spin polarized transport property often fails to go hand in hand with the ferromagnetic behavior of the material. In this study, we studied the transport property of our samples together with their magnetic properties. We performed Hall measurement to look for anomalous spin polarized transport behavior. Anomalous Hall effect (AHE) was clearly observed. Figure 5 shows the measured Hall resistance (at room temperature) as a function of the magnetic field from -1 T to 1 T for a 2% Mn sample. To correlate the AHE behavior with the

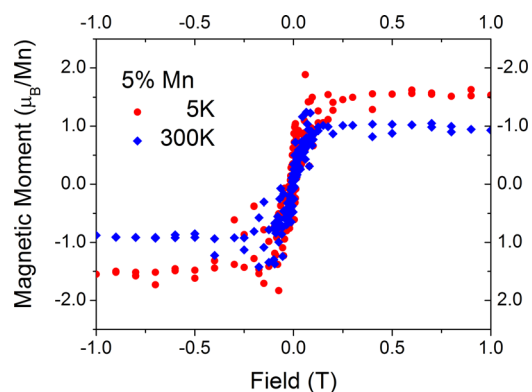


FIG. 3. Field dependent magnetization for a 5% Mn sample at 5 K and 300 K. The magnetization, expressed in number of Bohr magneton per Mn ion, was obtained by dividing the measured magnetization by the total dose of the implanted Mn atoms. The saturated moment is $1.58 \mu_B$ at 5 K and $1.03 \mu_B$ at 300 K, and magnetization reached saturation around 0.15 T.

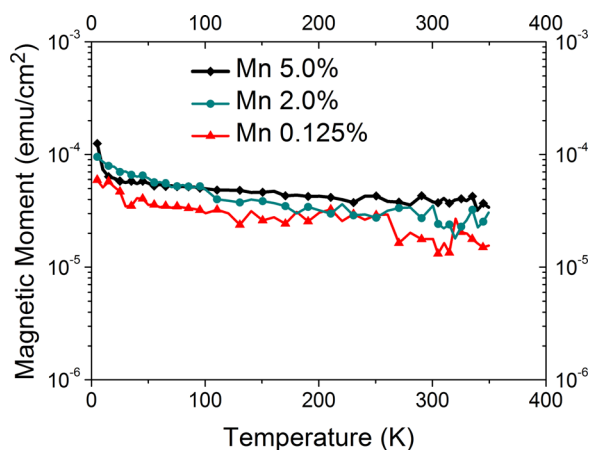


FIG. 4. Temperature dependence of the remnant magnetization for samples with Mn concentration: 0.125%, 2%, and 5%.

magnetization of the material, the measured field dependent magnetization is shown in the same figure. It should be mentioned that the background of the normal Hall effect due to the p-type doped Ge substrate was subtracted from the measured data to get the AHE signal. The field dependent magnetization and the AHE behavior correlate with each other perfectly. They have similar saturation behavior and saturate at the same field strength (+0.15 T). The AHE behavior was observed from 20 K to 300 K (the lowest temperature of 20 K was due to instrumentation limitation). The fact that the AHE correlates with the ferromagnetic behavior clearly indicates that the spin polarized carriers that are responsible for current transport are directly related to the ferromagnetic property of the material.

The ferromagnetism of GeMn has been postulated by RKKY model²⁶ as a result of magnetic moment coupling of Mn atoms mediated by holes. We have performed XMCD to study the electronic structure of doped Mn ions and the origin of ferromagnetism. The 2p-XAS and XMCD signals of the samples were measured either with total electron yield (TEY) or total fluorescence yield (TFY). Here the energy resolution of synchrotron radiation was set to 0.4 eV. Figure 6 shows the TFY of XMCD for the 2p-3d transitions of Mn. The measurement was carried out at 78 K for the sample

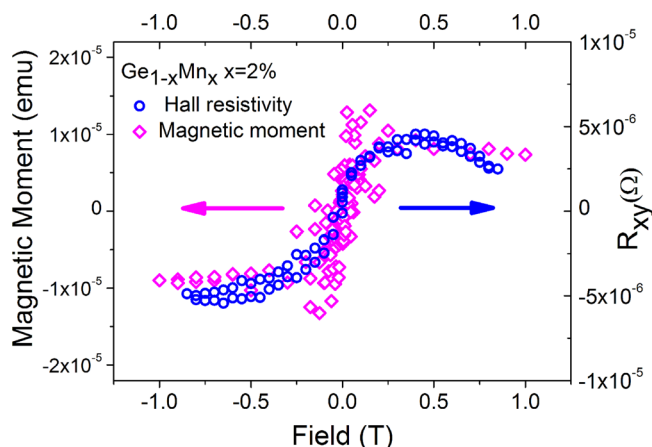


FIG. 5. Comparison between magnetization moment (emu) and Hall resistivity (R_{xy}) curves with magnetic fields from -1 T to 1 T. The signal is scaled for visibility.

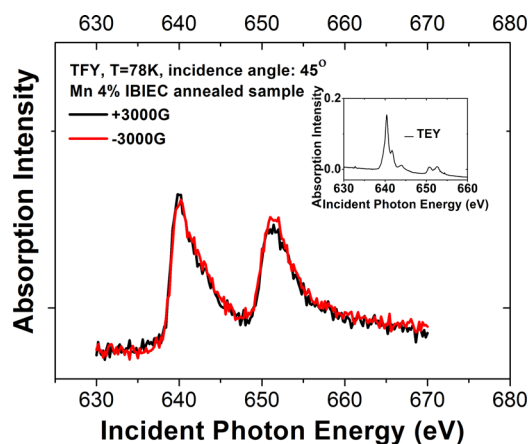


FIG. 6. Experimental Mn 2p-XAS spectra of the $\text{GeMn}_{0.04}$ measured at 78 K, the MCD signal can be obtained from the difference in the spectra. The inset shows the total electron yields of the 2p-XAS spectrum.

with 4% Mn. The difference in the XAS spectra at $2p_{1/2}$ and $2p_{3/2}$ obtained by excitations from opposite circularly polarized light indicates that the origin of ferromagnetism is indeed from the unpaired d shell electrons of Mn atoms. The characteristics of the 2p-XAS spectrum were also used to assess the electronic valence state of Mn ions in the Ge matrix. From the $2p_{3/2}$ peak positions in TEY and the sharp peaks of TEY (see inset) we may infer that the electronic valence state was 2^+ . This state also indicates that Mn ions are on the substitutional sites in the Ge lattice. These results presented above also provide evidence that the Mn ions serve as acceptors in Ge and the free holes are spin polarized to carry the magnetic property of the material.

We have estimated the percentage of Mn atoms that are ferromagnetic in our samples. The saturated magnetic moment divided by the total number of implanted Mn atoms gives the average magnetic moment per atom. Since a fully magnetized Mn atom has $2.5\mu_B$,²⁷ the ratio of the average magnetic moment per atom and $2.5\mu_B$ gives the percentage of ferromagnetic Mn atoms. For the 5% Mn sample, the estimated magnetization ratio is 63%. This number is significantly higher than what has been reported for Mn-implanted Ge films with conventional annealing techniques.^{10,17,19,25}

In summary, we have prepared ferromagnetic GeMn films using Mn implantation and IBIEC annealing. He irradiation was found to be very effective in removing damage caused by ion-implantation. Several structural analyses were carried out and showed that the Mn ions were uniformly incorporated into the Ge lattice without the formation of secondary phases. The ferromagnetic property along with the anomalous Hall effect was measured at room temperature. The 2p-XAS measurements showed that Mn ions were incorporated in the substitutional sites of the Ge lattice with 2^+ state. The correlation of the magnetic behavior and the transport behavior, along with the XMCD result, provides direct evidence that the spin polarized transport is directly related to the ferromagnetic property of the GeMn film. With our IBIEC technique, a very high magnetization ratio of 63% for the Mn ions was obtained. This study showed that IBIEC is a very valuable tool in repairing damages for thin films prepared in a non-equilibrium process. It is particularly useful for the fabrication of DMS thin films, where the magnetic

impurities need to be incorporated into the host material beyond the solid solubility.

This work was supported by the National Science Council under Grant Nos. NSC-99-2120-M-009-009, NSC-100-2120-M-009-005, and NSC-100-2221-E-007-124.

- ¹H. Munekata, H. Ohno, S. von Molnar, A. Segmüller, L. L. Chang, and L. Esaki, *Phys. Rev. Lett.* **63**(17), 1849 (1989).
- ²H. Ohno, A. Shen, F. Matsukura, A. Oiwa, A. Endo, S. Katsumoto, and Y. Iye, *Appl. Phys. Lett.* **69**(3), 363 (1996).
- ³Y. D. Park, A. T. Hanbicki, S. C. Erwin, C. S. Hellberg, J. M. Sullivan, J. E. Mattson, T. F. Ambrose, A. Wilson, G. Spanos, and B. T. Jonker, *Science* **295**(5555), 651 (2002).
- ⁴S. Cho, S. Choi, S. C. Hong, Y. Kim, J. B. Ketterson, B.-J. Kim, Y. C. Kim, and J.-H. Jung, *Phys. Rev. B* **66**(3), 033303 (2002).
- ⁵F. Tsui, L. He, L. Ma, A. Tkachuk, Y. S. Chu, K. Nakajima, and T. Chikyow, *Phys. Rev. Lett.* **91**(17), 177203 (2003).
- ⁶D. Bougeard, N. Sircar, S. Ahlers, V. Lang, G. Abstreiter, A. Trampert, J. M. LeBeau, S. Stemmer, D. W. Saxey, and A. Cerezo, *Nano Lett.* **9**(11), 3743 (2009).
- ⁷M. Jamet, A. Barski, T. Devillers, V. Poydenot, R. Dujardin, P. Bayle-Guillemaud, J. Rothman, E. Bellet-Amalric, A. Marty, J. Cibert, R. Mattana, and S. Tatarenko, *Nat. Mater.* **5**(8), 653 (2006).
- ⁸J. Ye, Y. Jiang, Q. Liu, Y. Sun, Z. Pan, and S. Wei, *J. Phys.: Conf. Series* **190**(1), 012104 (2009).
- ⁹L. Ottaviano, M. Passacantando, S. Picozzi, A. Continenza, R. Gunnella, A. Verna, G. Bihlmayer, G. Impellizzeri, and F. Priolo, *Appl. Phys. Lett.* **88**(6), 061907 (2006).
- ¹⁰S. Zhou, D. Bürger, A. Mücklich, C. Baumgart, W. Skorupa, C. Timm, P. Oesterlin, M. Helm, and H. Schmidt, *Phys. Rev. B* **81**(16), 165204 (2010).
- ¹¹S. Sugahara, K. L. Lee, S. Yada, and M. Tanaka, *Jpn. J. Appl. Phys.* **44**, L1426 (2005).
- ¹²L. Ottaviano, M. Passacantando, A. Verna, R. Gunnella, E. Principi, A. Di Cicco, G. Impellizzeri, and F. Priolo, *J. Appl. Phys.* **100**(6), 063528 (2006).
- ¹³S. Zhou, *Appl. Phys. Lett.* **95**(19), 192505 (2009).
- ¹⁴S. Zhou and H. Schmidt, *Materials* **3**(12), 5054 (2010).
- ¹⁵Y. Wang, *Appl. Phys. Lett.* **92**(10), 101913 (2008); D. D. Dung, W. Feng, Y. Shin, and S. Cho, *J. Appl. Phys.* **109**(7), 07C310 (2011).
- ¹⁶L. T. Yoon, C. J. Park, S. W. Lee, T. W. Kang, D. W. Koh, and D. J. Fu, *Solid-State Electronics* **52**(6), 871 (2008).
- ¹⁷W. Yin, L. He, M. C. Dolph, J. Lu, R. Hull, and S. A. Wolf, *J. Appl. Phys.* **108**(9), 093919 (2010).
- ¹⁸M. A. Scarpulla, U. Daud, K. M. Yu, O. Monteiro, Z. Liliental-Weber, D. Zakharov, W. Walukiewicz, and O. D. Dubon, *Phys. B: Condens. Matter* **340–342**(0), 908 (2003).
- ¹⁹S. Zhou, D. Burger, W. Skorupa, P. Oesterlin, M. Helm, and H. Schmidt, *Appl. Phys. Lett.* **96**(20), 202105 (2010).
- ²⁰C. H. Chen, H. Niu, H. H. Hsieh, C. Y. Cheng, D. C. Yan, C. C. Chi, J. J. Kai, and S. C. Wu, *J. Magn. Magn. Mater.* **321**(9), 1130 (2009).
- ²¹S. T. Johnson, J. S. Williams, E. Nygren, and R. G. Elliman, *J. Appl. Phys.* **64**(11), 6567 (1988).
- ²²C. H. Chen, H. Niu, H. H. Hsieh, J. W. Chiou, and C. P. Lee, “XAFS Study on Mn-implanted Ge treated by IBIEC” (unpublished).
- ²³J. Chen, Kang L. Wang, and K. Galatsis, *Appl. Phys. Lett.* **90**(1), 012501 (2007).
- ²⁴A. Verna, L. Ottaviano, M. Passacantando, S. Santucci, P. Picozzi, F. D’orazio, F. Lucari, M. De Biase, R. Gunnella, M. Berti, A. Gasparotto, G. Impellizzeri, and F. Priolo, *Phys. Rev. B* **74**(8), 085204 (2006).
- ²⁵M. C. Dolph, T. Kim, W. Yin, D. Recht, W. Fan, J. Yu, M. J. Aziz, J. Lu, and S. A. Wolf, *J. Appl. Phys.* **109**(9), 093917 (2011).
- ²⁶M. J. Calderón and S. Das Sarma, *Ann. Phys.* **322**(11), 2618 (2007).
- ²⁷T. C. Schulthess and W. H. Butler, *J. Appl. Phys.* **89**(11), 7021 (2001).
- ²⁸F. Matsukura, A. Oiwa, A. Shen, Y. Sugawara, N. Akiba, T. Kuroiwa, H. Ohno, A. Endo, S. Katsumoto, and Y. Iye, *Appl. Surf. Sci.* **113–114**, 178 (1997).
- ²⁹H. Ohno, *Science* **281**(5379), 951 (1998).
- ³⁰O. Riss, A. Gerber, I. Ya Korenblit, A. Suslov, M. Passacantando, and L. Ottaviano, *Phys. Rev. B* **79**(24), 241202 (2009).
- ³¹C. P. Z. Werner, M. Barlak, J. Piekoszewski, A. Korman, R. Heller, W. Szymczyk, and K. Bocheńska, *Nukleonika* **56**(1), 4 (2011).
- ³²C. T. Chen, F. Sette, Y. Ma, and S. Modesti, *Phys. Rev. B* **42**(11), 7262 (1990).
- ³³G. van der Laan and B. T. Thole, *Phys. Rev. B* **43**(16), 13401 (1991).
- ³⁴See supplementary material at <http://dx.doi.org/10.1063/1.4729752> for microstructure and magnetic properties evidenced by HRTEM, SIMS, and SQUID of as-implanted and IBIEC annealed samples.